FEBS Letters

FEBS PRESS science publishing by scientists

Interplay of SpkG kinase and the Slr0151 protein in the phosphorylation of ferredoxin 5 in *Synechocystis* sp. strain PCC 6803

Martina Angeleri[1], Anna Zorina[2], Eva-Mari Aro[1] and Natalia Battchikova[1]

1 Molecular Plant Biology, Department of Biochemistry, University of Turku, Finland
2 Institute of Plant Physiology, Laboratory of Intracellular Regulation, Russian Academy of Sciences, Moscow, Russia

Correspondence
N. Battchikova, Molecular Plant Biology, Department of Biochemistry, University of Turku, FI-20014, Turku, Finland
Fax: +358-29-4505040
Tel: +358-2-3338078
E-mail: natbat@utu.fi

(Received 9 November 2017, revised 29 December 2017, accepted 2 January 2018, available online 1 February 2018)

doi:10.1002/1873-3468.12970

Edited by Miguel De la Rosa

In *Synechocystis* 6803, the ferredoxin 5 (Fd5) phosphoprotein and the S/T protein kinase SpkG are encoded by the *slr0148* and *slr0152* genes, respectively, which belong to the *slr0144–slr0152* cluster. Using a targeted proteomic approach, we showed that SpkG is responsible for the phosphorylation of Fd5 on residues T18 and T72. Sequence alignments and Fd5 structure modelling suggest that these phosphorylation events modulate protein–protein interaction. Furthermore, Fd5 phosphorylation is affected by the Slr0151 protein encoded by the gene preceding *spkG* in the gene cluster. We propose that Slr0151 functions as an auxiliary protein in the regulation of the ratio between phosphorylated and nonphosphorylated forms of Fd5.

Keywords: ferredoxin 5 phosphoprotein; S/T phosphorylation; SpkG protein kinase

Reversible protein phosphorylation is essential for the regulation of most vital aspects of cell function, like cell growth, division and differentiation, in both prokaryotes and eukaryotes [1–3]. Research based on the phosphoproteomic approaches [4] has demonstrated that the eukaryotic type of protein phosphorylation, namely modification of Ser, Thr and Tyr residues (S/T/Y- or O-phosphorylation), occurs also in bacterial species [5]. Cyanobacteria are prokaryotic microorganisms able to perform oxygenic photosynthesis, that is, transforming energy of sunlight into chemical energy (ATP and NADPH) by splitting water molecules and releasing oxygen. Recent phosphoproteomic investigations of cyanobacteria revealed hundreds of S/T/Y phosphoproteins participating in a wide spectrum of biological functions including photosynthesis and other processes connected with the intracellular energy tranfer [6–9].

While the knowledge on occurrence of S/T/Y phosphoproteins in cyanobacteria has increased dramatically in the past few years, very limited information is available about interactions between cyanobacterial protein kinases and their target phosphoproteins [10–12]. In the genome of the model unicellular cyanobacterium *Synechocystis* sp. PCC6803 (hereafter *Synechocystis* 6803), seven genes, *spkA–spkG*, have been predicted to encode for the S/T protein kinases of the Pkn2 family, and five genes, *spkH–spkL*, for the ones of the ABC1 family [13,14]. SpkA is involved in the control of cell motility by regulating expression of

Abbreviations
ABC, ammonium bicarbonate; AcN, acetonitrile; DDA, data-dependent acquisition; FA, formic acid; Fd, ferredoxin; HCD, high-energy collision dissociation; IAA, iodoacetamide; Km-R, kanamycin resistance cassette; LC-MS/MS, liquid chromatography–tandem mass spectrometry; MS, mass spectrometry; nCE, normalized collision energy; OV, sodium orthovanadate; PAP, photosystem II assembly proteins; PBS, phycobilisomes; PSII, photosystem II; PTM, post-translational modification; RT, room temperature; RT-qPCR, RT quantitative PCR; SRM, selected reaction monitoring; TCEP, tris(2-carboxyethyl)phosphine hydrochloride; TPRs, tetratricopeptide repeats; TSQ, triple-stage quadrupole; WT, wild-type.

pili family genes [15,16]. SpkB seems to be also involved in motility, but details of its role in this function and the interaction with SpkA remain unclear [17]. SpkE is probably involved in the regulation of nitrogen metabolism [18], while SpkG was shown to play role in salt stress response, positively regulating expression of 15 genes [19]. Zorina *et al.* [14] demonstrated that SpkC, SpkF and SpkK are involved in phosphorylation of the small chaperonin GroES. However, regulation, function, and substrate recognition of *Synechocystis* 6803 S/T protein kinases remain poorly investigated [13]. In particular, the field is lacking studies directed to establishing relationships between a discrete S/T protein kinase and individual phosphorylation site(s) in various phosphoproteins of *Synechocystis* 6803 and other cyanobacteria.

In *Synechocystis* 6803, SpkG protein kinase is encoded by the *slr0152* gene which belongs to the cluster of nine genes, *slr0144–slr0152,* located closely to each other. The cluster has been described as the photosystem II assembly proteins (PAP) operon [20]. Later, Mitchke *et al.* [21]. showed that *slr0151* and *slr0152* are transcribed separately from the upstream genes, possibly as bicistronic mRNA. Among other proteins, the *slr0144–slr0152* gene cluster encodes the Slr0148 protein which has been recently annotated as ferredoxin 5 (Fd5) [22] and shown to be a phosphoprotein, with modified T18 and T72 [7] residues [7,9]. Here, we demonstrate a relationship between phosphorylation of Fd5 and the SpkG kinase which was revealed by investigation of the *Δslr0152(ΔspkG)* mutant of *Synechocystis* 6803 with the targeted proteomic approach (the selected reaction monitoring, SRM). Moreover, we show that the knockout of *slr0151*, the gene encoding the protein with the tetratricopeptide repeat (TPR) motif and preceding *spkG* in the operon, caused the increase in Fd5 phosphorylation. The demonstrated interplay of three proteins, Fd5 (Slr0148), Slr0151 and the SpkG kinase (Slr0152), exposes a complexity of S/T protein phosphorylation network in *Synechocystis* 6803.

Materials and methods

Culture conditions

Wild-type (WT) and mutant *Synechocystis* 6803 cells were grown in BG-11 medium [23] buffered with HEPES-NaOH (10 mM, pH 7,5) in flasks shaking at 120 rpm in air, at 30 °C. Solid medium was the same BG-11 supplemented with 1.5% agar. Continuous illumination was provided by fluorescent lamps at 50 μmol photons^{-2}·s^{-1} for approximately 5 days, until OD_{750} ~ 1. For selection and storage, mutants were kept on solid medium with 50 mg·L^{-1} kanamycin (Km).

Construction of *slr0152* (*spkG*) and *slr0151* mutants

The glucose-tolerant WT *Synechocystis* 6803 strain was used for construction of Δ*slr0152* and Δ*slr0151* mutants. The *slr0152* (*spkG)* ORF was disrupted by insertion of the kanamycin resistance cassette (Km-R) into the native PstI site of *slr0152*. To that, the *Synechocystis* 6803 DNA fragment was amplified by PCR using primers 1 and 2 (Table 1). After digestion with HindIII and NdeI, the PCR fragment was inserted in the pRSET-A vector (Invitrogen) and cloned in *Escherichiea coli*. Furthermore, the Km-R cassette was inserted into the unique PstI site of the obtained plasmid. The final construct was used for the generation of the *Synechocystis* 6803 *Δslr0152* mutant by the homologous recombination. The *Synechocystis* 6803 *Δslr0151* mutant was produced by replacing the part of ORF encoding Asn15-Gln145 with Km-R. The upstream region was amplified by PCR using primers 3 and 4 with introduced EcoRI and PstI sites respectively (Table S1). The downstream region was amplified by PCR using the primer 5 with introduced PstI site and the primer 6 (Table S1). The former PCR fragment was digested with EcoRI and PstI, the latter one with PstI and BamHI (the native site in the chromosomal DNA), and both were inserted into the pRSET-A/EcoRI-BamHI vector and cloned in *E. coli*. After the Km-R cassette was inserted into PstI site, the *Synechocystis* 6803 *Δslr0151* mutant was generated as described above. Complete segregation in mutants was confirmed by PCR with primers 1 and 2 for *Δslr0152* and primers 3 and 7 for *Δslr0151*.

Real-time quantitative PCR

RNA isolation and cDNA synthesis were performed as described in Mustila *et al.* [24]. The RT quantitative PCR (RT-qPCR) was performed on a Bio-Rad IQ5 system using iQ SYBR Green Supermix (Bio-Rad Laboratories, Hercules, CA, USA). WT and Δ*slr0151* were analysed in triplicates. Melting curve analysis was performed after 40 cycles of PCR for each run to ensure the specificity of the expected amplicon product. *rnpB* was used as a reference gene [25]. The primers 8 and 9 used for RT-qPCR are shown in Table S1.

Protein isolation and digestion to peptides

For quantitative proteomic experiments, WT and mutant strains were grown to OD_{750} ~ 1 without the antibiotic. Cultures were collected by centrifugation at 6500 ***g*** for 10 min at 4 °C and washed by resuspension in ice-cold deionized water followed by centrifugation in the same

Table 1. Changes in protein expression and phosphorylation in Δ*slr0151* and Δ*spkG* mutants. Relative changes for individual peptides have been calculated in percentage compared to WT from the SRM results presented in the Table S3. Statistically significant changes for three biological replicates are marked by stars. N/A: a ratio has not been calculated because a peptide was not detected in one of the strains.

	Δ*slr0151*/WT	Δ*slr0152*/WT
Slr0148		
VAIETNDNLLSGLLGQDLR	79%*	131%*
VAIE**pT**NDNLLSGLLGQDLR	189%*	17%*
TLEVITTHNR	93%	160%*
TLEVIT**pT**HNR	147%*	N/A
LDPIDLK	86%*	104%
DGSILVEK	84%*	105%
SMISQLDDQLQAAK	83%*	111%
Slr0151		
FQGDIQTSLGQQQQAIAANQENLTK	N/A	45%*
LYFDQGDLDSYEVAR	N/A	48%*
Slr2067		
SIVNADAEAR	102%	105%
Sll1577		
ITGNASAIVSNAAR	102%	113%*
ITGNAS**pT**AIVSNAAR	87%	110%

conditions. Cells were resuspended in a denaturing buffer A containing 0.1 M ammonium bicarbonate (ABC), 9 M urea, 5 mM EDTA, 5 mM EGTA, 1 mM PMSF, 20 mM NaF, 5 mM $Na_4P_2O_7$, 20 mM glycerol 2-phosphate. Cells were broken using zirconium beads (0.15 mm, 5.5 g·cc^{-1}, 1 lb, NextAdvanace- cat.no. ZROB015) in a Bullet Blender® Homogenizers (Next Advance, Inc., Troy, NY, USA), applying three 5-min pulses with maximum power. The crude extract was supplemented with 1% sodium deoxycholate monohydrate (Sigma-Aldrich Corporation, St. Louis, MO, USA) and incubated for 10 min at room temperature (RT). Cell debris was removed by centrifugation at 21 000 ***g*** for 30 min at RT. Protein concentration was measured using Pierce™ BCA Protein Assay Kit (cat.no. 23225; Thermo Fisher Scientific, Waltham, MA, USA). For each sample, an aliquot corresponding to 1.3 µg of proteins was adjusted to the 250-µL volume with the buffer A followed by reduction of disulphide bonds with 10 mM tris(2-carboxyethyl)phosphine hydrochloride (TCEP) and alkylation with 50 mM iodoacetamide (IAA) for 30 min at RT in the dark. Proteins were precipitates with five volumes of the ice-cold acetone : ethanol (1 : 1) solution at −20 °C overnight. Furthermore, proteins were dissolved in the buffer B (50 mM Tris-HCl pH 7.5, 5 mM NaF, 5 mM $Na_4P_2O_7$, 5 mM glycerol 2-phosphate) containing 8 M urea, diluted four times to decrease concentration of urea followed by addition of sodium orthovanadate (OV; 5 mM), $CaCl_2$ (1 mM) and TCPK-trypsin (cat.no. 20233; Thermo Scientific) in a ratio 1 : 25 w/w to the total protein. Digestion was performed at 30 °C overnight. Tryptic peptides were acidified with formic acid (FA) to pH 2–3 and desalted using C18 cartridges (Sep-Pak Vac 3 cc, 500 mg; Waters Corporation, Milford, MA, USA) equilibrated with 5% FA. After washing with 5% FA, C18-bound peptides were eluted with 80% acetonitrile (AcN) in 5% FA and dried in a SpeedVac concentrator SVC 100 (Savant Instruments Inc., Holbrook, NY, USA). Peptides were dissolved in 250 µL of 1% FA, and their amounts were estimated using Nanodrop ND-1000 (Thermo Scientific) and the Pierce™ BCA Protein Assay Kit (cat.no. 23225; Thermo Scientific).

LC−MS/MS analysis and SRM quantification

Selected reaction monitoring assays for the two phosphopeptides of Fd5 (Slr0148) and the CpcB phosphopeptides were described earlier in Angeleri *et al.* [9]. For the non-modified peptides, the SRM assays were designed as follows. The WT tryptic digest was analysed by liquid chromatography–tandem mass spectrometry (LC-MS/MS) in a data-dependent acquisition (DDA) mode using a Q Exactive™ Hybrid Quadrupole-Orbitrap mass spectrometer (Thermo Scientific) connected in-line with an Easy-nLC HPLC system (Thermo Scientific). Peptides were separated on a C18 precolumn (5 × 0.3 mm, PepMap C18, LC Packings) and a C18 nano-column (15 cm × 75 µm, Magic 5 µm200 Å C18; Michrom BioResources Inc., Sacramento, CA, USA) with a flow rate of 300 nL·min^{-1}, using 0.1% FA, 2% AcN as a buffer A and 0.1% FA, 95% AcN as a buffer B. A 60-min gradient was applied: from 5% to 26% B for 35 min, from 26% to 43% B for 15 min, 43% to 100% B for 2 min followed by 100% B for 10 min. Mass spectrometer equipped with an electrospray ionization source was operated in the positive ion mode, with ionization voltage of 2300 V. DDA was carried out using the following parameters: MS survey scans were performed in a mass range of 300–2000 *m*/*z* with resolution of 17 000. Precursor ions corresponding to peptides of interest were fragmented by high-energy collision dissociation (HCD) with the normalized collision energy (nCE) value of 30 eV, isolation window was 2.0 *m*/*z*, MS/MS ion scans were collected in a mass range of 100–2000 *m*/*z* with resolution of 17 500, with a 6-sec dynamic exclusion of an ion for fragmentation. The obtained data were analysed using the in-house MASCOT 2.4 (Matrix Science, London, UK) server via Proteome Discoverer 1.4 (ThermoFisher Scientific) as described in Angeleri *et al.* [9]. The data obtained by DDA LC-MS/MS were used as the peptide spectral library for designing of SRM assays for the peptide of interest. Q1/Q3 transitions were generated using SKYLINE software version 3.1.

Selected reaction monitoring experiments were performed on a triple-stage quadrupole (TSQ) Vantage mass spectrometer (Thermo Scientific) connected in-line with an Easy-nLC HPLC system (Thermo Scientific). The HPLC conditions for peptide separation were the same as in DDA LC-MS/MS. The TSQ Vantage mass spectrometer was operated in the positive ion mode with a capillary temperature of 270 °C, spray voltage of +1600 V and collision gas pressure of 1.2 mTorr. Q1 and Q3 peak width (FWHM) parameters were set to 0.7 and cycle time to 2.5 s; minimal dwell time was 30 ms. The resulting raw files were analysed by SKYLINE software version 3.1 [26]. Relative quantification of peptides in mutants in comparison to WT was based on calculated integrated peak areas obtained by summarizing the intensities of peptide-specific Q1/Q3 transitions. Statistically significant differences between WT and each of the mutant were evaluated using the two-tailed *T*-test.

Alignment and 3D structure of Slr0148

Primary sequence of Slr0148 protein was aligned to other *Synechocystis* 6803 ferredoxin proteins or to orthologous proteins in other cyanobacteria using the CLUSTAL OMEGA suit (https://www.ebi.ac.uk/Tools/msa/clustalo/) and BIOEDIT, version 7.2.5 [27]. Accession numbers of protein sequences correspond to Cyanobase (http://genome.microbedb.jp/cyanobase). The 3D model was constructed using Swiss Model from the Expasy suit (https://swissmodel.expasy.org/) and modified using the PYMOL Molecular Graphics System, Version 2.0 (Schrödinger, LLC, Portland, OR, USA).

Results

Δ*slr0152(spkG)* and Δ*slr0151* mutants of *Synechocystis* 6803

To investigate the hypothesis about an interplay of the SpkG protein kinase and phosphorylated Fd5 encoded in the same *slr0144–0152* gene cluster, we constructed the Δ*slr0152* mutant of the glucose-tolerant *Synechocystis* 6803. The cloning scheme is presented in Fig. 1. The *slr0152* gene was interrupted by insertion of the Km-R cassette into the natural PstI site. In parallel, we constructed another mutant where the part of *slr0151*, the gene which precedes *spkG* in the operon, was replaced with the Km-R cassette (Fig. 1). The latter mutant was deficient in the Slr0151 protein containing TPRs known to be involved in protein–protein interactions [28]. The complete segregation of both mutants was confirmed by PCR (Fig. S1A,B).

Design of SRM assays for quantification of selected proteins including Fd5 and Slr0151

To inspect the phosphorylation level of Fd5 in WT and constructed mutants, we applied SRM [29], the targeted LC-MS/MS quantification approach. Earlier we have shown that phosphorylation of Fd5 occurs on T18 and T72 residues [9]. The SRM assays for VAIE**pT**NDNLLSGLLGQDLR and TLEVI**pT**THNR phosphopeptides which incorporate T18 and T72 were described in Angeleri *et al*. [9]. These assays, which have been designed for verification of the Fd5, were ready for quantification experiments. Here, we designed SRM assays for the corresponding nonmodified peptides. The Q1/Q3 transitions based on the most intensive and selective fragment y ions in DDA spectra easily distinguished these peptides in the tryptic digest of the *Synechocystis* 6803 proteome in the SRM experiments. The retention time values and the characteristic transition groups for the two Fd5 peptides, in phosphorylated and nonphosphorylated forms, are shown in Fig. 2. Similarly, we designed the SRM assays for several other peptides originated from Fd5 (LDPIDLK, DGSILVEK and SMISQLDDQLQAAK) and Slr0151 (FQGDIQTSLGQQQQAIAANQENLTK and LYFDQGDLDSYEVAR) to monitor the general expression level of these proteins (Skyline file in Doc. S1). We attempted also to make SRM assays for several peptides from SpkG. However, we could not reliably detect any of them in the proteome digest, most probably due to the low abundance of SpkG in the *Synechocystis* 6803 proteome. Finally, we designed SRM assays for peptides from phycobilisome (PBS) subunits: SIVNADAEAR (ApcA, Slr2067) and ITGNASAIVSNAAR (CpcB, Sll1577; Skyline file in Doc. S1). Latter peptides represented proteins independent on the PAP operon and were used as controls. The designed SRM assays were submitted to Panorama Public, https://panoramaweb.org.

Distinct phosphorylation of Fd5 in *spkG* and *slr0151* knockout mutants

Preliminary experiments demonstrated that both VAIE**pT**NDNLLSGLLGQDLR and TLEVI**pT**THNR phosphopeptides of Fd5 were abundant in WT cells. Therefore, the quantification was performed on samples comprising the total peptide mixture after trypsin digestion of the proteome, without the TiO_2 enrichment [4]. Three samples prepared from independently grown cell cultures were assessed for every strain. The results of SRM runs are presented in the Skyline file in Doc. S1. The expression level of a peptide in a sample was estimated as the integrated peak area for all measured transitions of the peptide (Table S2). Average values (for the 3 biological replicas) were normalized to the amounts of peptides present in WT (Table S3).

Results of relative quantification, with standard deviations, are shown in Figs 3 and 4 and Table 1. They revealed the absence of the TLEVI**pT**THNR

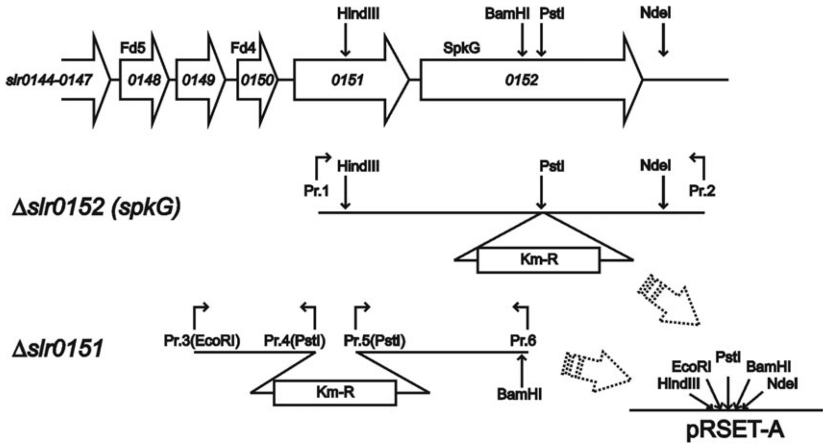

Fig. 1. The cloning scheme for the construction of the Δ*slr0152* and Δ*slr0151* mutants of the glucose-tolerant *Synechocystis* 6803 strain.

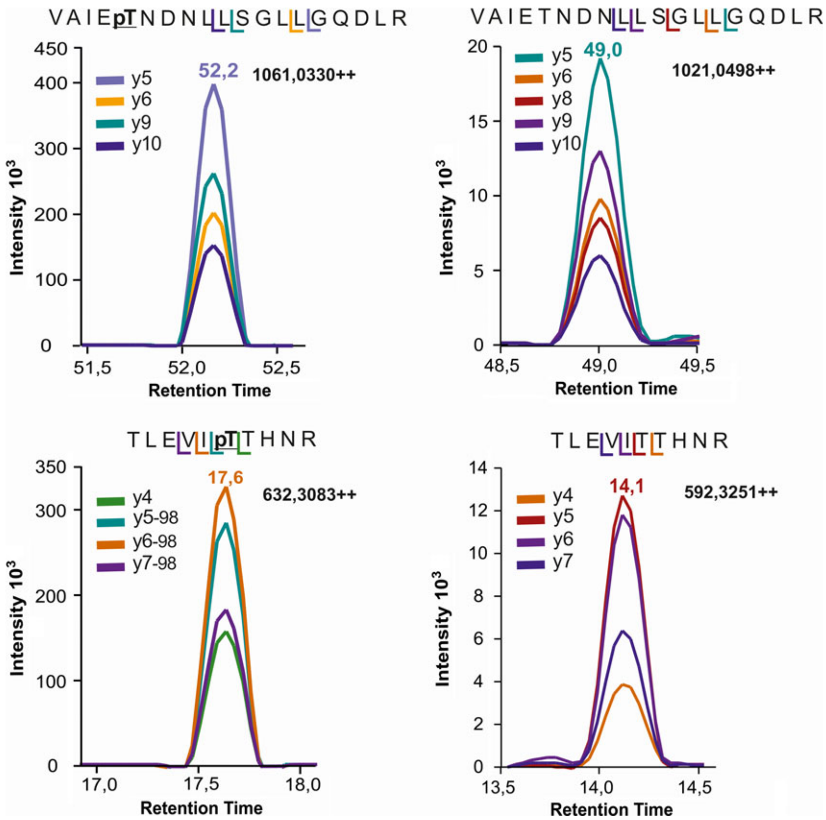

Fig. 2. Characteristic Q1/Q3 transition groups used to quantify the phosphorylated and nonmodified tryptic peptides of Fd5 using the SRM approach. Corresponding mass-to-charge values are shown on the right side. Individual product ions are depicted by different colours.

phosphopeptide and the dramatic decrease in the VAIE**pT**NDNLLSGLLGQDLR amounts in the Δ*slr0152* (Δ*spkG*) mutant. In accordance, enhanced accumulation of the corresponding nonphosphorylated peptides was observed in this strain. Unexpectedly, we detected increased amounts of both phosphopeptides in the Δ*slr0151* mutant compared to WT. The nonphosphorylated forms of the peptides slightly diminished in the Δ*slr0151* strain. Three peptides, LDPIDLK, DGSILVEK and SMISQLDDQLQAAK, were monitored as reporters for general protein level of Fd5. The obtained data (Fig. 4A) showed that the *slr0152* deletion and consequent elimination of the SpkG kinase did not affect the Fd5 protein expression/accumulation. In the Δ*slr0151* mutant, the Fd5 protein production was reduced about 15% compared to WT. Furthermore, two peptides, FQGDIQTSLGQQQQAIAANQENLTK and LYFDQGDLDSYEVAR, served as controls for the Slr0151 protein expression (Fig. 4B). As expected, the Slr0151 protein was absent in the Δ*slr0151* mutant confirming results of the segregation analysis. Surprisingly, insertion of the Km-R cassette in the middle of the following *slr0152* gene and abolishing of the SpkG kinase reduced the expression of Slr0151 to about 50% compared to WT. It was important to test whether the *slr0151* deletion affected the expression of the SpkG. Since the SRM detection of the SpkG kinase was not possible, we performed RT-qPCR analysis of *slr0152* mRNA in WT and the Δ*slr0151* mutant. Results showed that insertion of the Km-R cassette into *slr0151* and, therefore, elimination of the Slr0151 production did not affect the expression of the downstream *slr0152* gene (Fig. S2). Last, the PBS peptides, SIVNADAEAR from ApcA, unmodified ITGNASAIVSNAAR and phosphorylated ITGNA**pS**AIVSNAAR from CpcB, were nearly similarly expressed in all three strains (Fig. 4C).

Sequence alignment and the 3D model suggest that Fd5 phosphorylation modifies protein–protein interaction

We performed primary sequence alignment of Fd5 from *Synechocystis* 6803 with orthologous proteins from other four cyanobacteria carrying the PAP operon in their genomes [20]. The alignment (Fig. S3) showed high similarity within the group and the threonines, which are phosphorylated in Slr0148, were strictly conserved.

To get insights into the physiological role of Fd5 phosphorylation, we made sequence alignment of Fd5 with plant-type 2Fe-2S ferredoxins 1–4 (Ssl0020, Sll1382, Slr1828 and Slr0150 respectively) of *Synechocystis* 6803. The alignment showed that both phosphorylated sites in Fd5 reside in the conserved ferredoxin domain of plant-type ferredoxins. It is important to note that the positions of T18 and T72 in Fd5 are occupied by negatively charged amino acids (D, E) in the other four ferredoxins (Fig. 5). Thus, phosphorylation of Fd5, leading to the introduction of negative charges on the matching positions, increased the homology of this protein with the group of the plant-type 2Fe-2S ferredoxins Fd1–Fd4, despite rather moderate general identity/similarity of Fd5 with these four proteins. In addition, the alignment showed the presence of another domain at the C terminus of Fd5 that is not present in other ferredoxins. It was annotated as RNA_pol_Rpb1_2 domain, but its functional importance in Fd5 remains unknown.

Furthermore, we performed modelling of Fd5 based on the 3D structure of putidaredoxin from *Pseudomonas putida* (4jws.1.B), which had the highest score of similarity to Fd5 of *Synechocystis* 6803 according to the Swiss Model program (Fig. 6A). Similarly, Fd5 was modelled based on the structure of *Synechocystis* 6803 Fd1 (1off.1.A) as a representative of the plant-

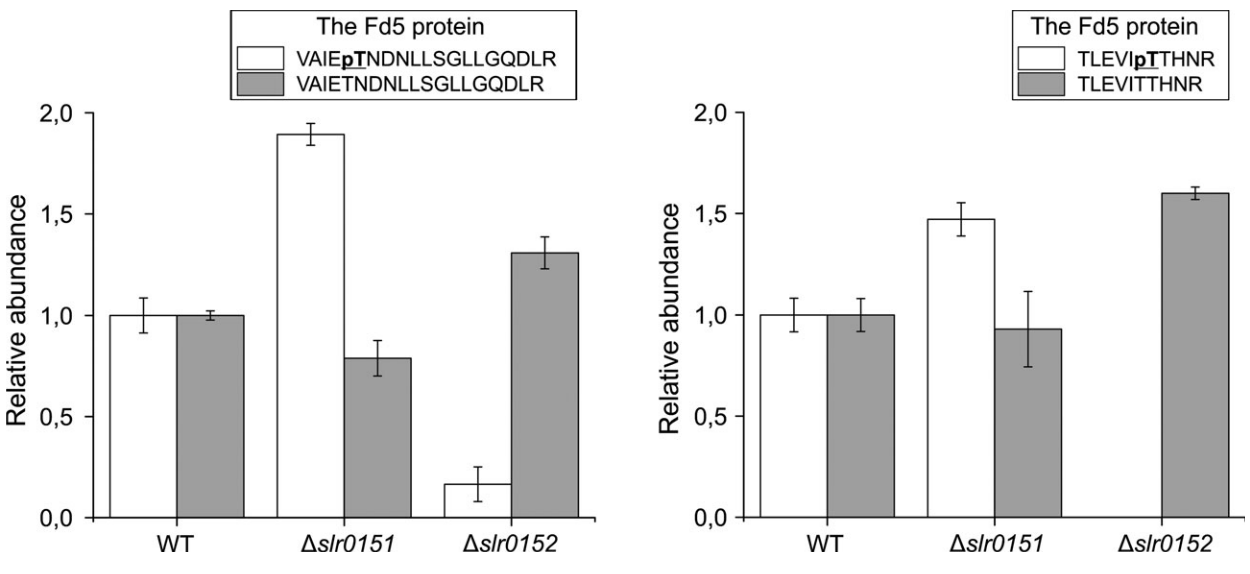

Fig. 3. Relative quantification of phosphorylated and nonphosphorylated form of VAIETNDNLLSGLLGQDLR and TLEVITTHNR peptides of Fd5 in WT, Δ*slr0152* and Δ*slr0151* mutants performed by SRM. The graph represents average values obtained for three biological replicates normalized to the amount of peptides present in WT. White bars correspond to phosphopeptides, grey bars – to the nonmodified peptides.

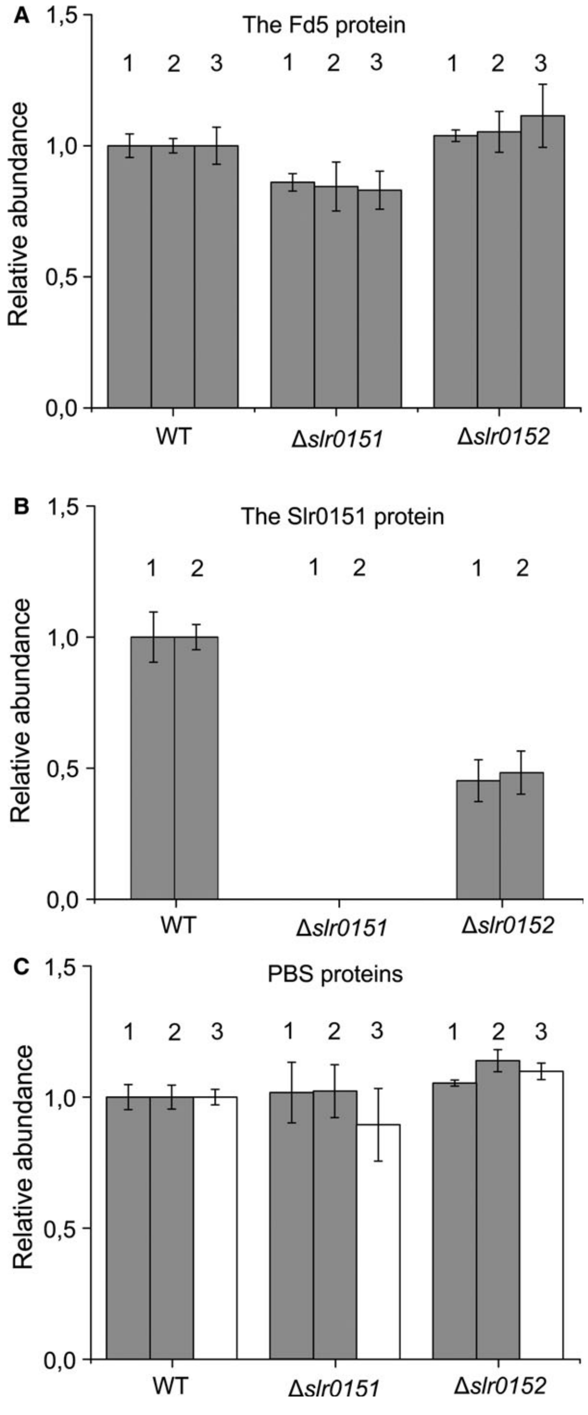

Fig. 4. Relative quantification of Fd5, Slr0151 and PBS expression in WT, the Δ*slr0152* and Δ*slr0151* mutants. The following peptides were assessed: (A) LDPIDLK (1), DGSILVEK (2), SMISQLDDQLQAA (3) for Fd5; (B) FQGDIQTSLGQQQQAIAANQENLTK (1), LYFDQGD LDSYEVAR (2) for Slr0151; (C) SIVNADAEAR from ApcA (1), ITGNASAIVSNAAR from CpcB in phosphorylated (2) and nonmodified (3) forms, for PBS proteins. Average values obtained for three biological replicates were normalized to the amount of peptides present in WT.

type 2Fe-2S ferredoxins in this organism (Fig. 6B). Although the reliability of the latter model remained questionable due to the low level of homology, both models predicted the location of phosphorylated residues on the opposite sides of the protein (Fig. 6A) implying possible effect on the protein–protein interactions.

Discussion

Recent phosphoproteomic studies [7–9] of the model unicellular cyanobacterium *Synechocystis* 6803 have revealed the occurrence of the eukaryotic type, S/T/Y, protein phosphorylations in many proteins involved in various cellular functions. This strongly suggests that cyanobacteria, like other organisms, exploit this post-translational modification (PTM) for regulation and signalling. However, the network of S/T protein kinases and corresponding phosphorylation sites in cyanobacterial proteins remains scarcely investigated.

In the current work, we studied a relationship between the S/T protein kinase SpkG and the Fd5 phosphoprotein, both encoded by the *slr0144–slr0152* gene cluster in *Synechocystis* 6803 [28]. To this end, the Δ*slr0152* mutant deficient in the SpkG kinase was constructed, and the targeted proteomic approach [29] was applied to evaluate the level of Fd5 phosphorylation in the mutant compared to WT. In parallel, the Δ*slr0151* mutant deficient in the TPR-containing Slr0151 protein, encoded by the gene preceding *spkG* in the gene cluster, was constructed and analysed. The SRM approach used here allows the relative quantification of an individual peptide in various samples but does not permit direct comparison of different peptides, due to their variant behaviour during MS data acquisition. Therefore, the results of the quantitative SRM analyses were normalized to the WT level for each peptide, and no quantitative ratio between phospho-Fd and the nonmodified protein is provided.

Ferredoxin 5 is phosphorylated on two sites, T18 and T72 [9], and both threonines are strictly conserved among corresponding proteins in other cyanobacteria possessing the PAP operon (Fig. S3). Targeted SRM investigation showed complete absence of T72 phosphorylation and drastically diminished T18 phosphorylation of Fd5 in the SpkG-deficient mutant Δ*slr0152* (Fig. 3 and Skyline file in Doc. S1). In accordance, levels of the corresponding nonmodified peptides increased in the Δ*slr0152* mutant. Since the absence of SpkG did not affect the general expression level of the Fd5 protein (Fig. 4A), it can be concluded that the SpkG kinase is indeed involved in phosphorylation of Fd5. The remaining low level of phosphorylation on

```
                 2Fe-2S cluster-binding domain
Fd 5  MAKTIKLDPI------DLKVAIETNDNLLSGLLGQDLRIMKECGGRGMCATCHVYITAGM
Fd 1  M-ASYTVKLITPDG--ESSIECSDDTYILDAAEEAGLDLPYSCR-AGACSTCAGKITAGS
Fd 2  MSRSHRVLIHDRQNEKDYSVIVSDDRYILHQAEDQGFELPFSCR-NGACTACAVRVISGQ
Fd 3  MVNTYTAEIQHQGQ--TYTISVPEDKTVLQAADDEGIQLPTSCG-AGVCTTCAALITEGT
Fd 4  MGAIYSVNLVNPATGSDVTIEVAEDELILEAAENQGLDLPYSCR-AASCVACAGRLLEGT
      *                 .:    :  :*      .:    .*   . * :*   :  *

Fd 5  ESLSPLNRREQRTLEVITTHNRYSRLACQARVLDEGVVVELPAGMYVSEIEDIEELIGRR
Fd 1  VDQSDQ------SFLDDDQIEAGYVLTCVAYPTSDCTIETHK--------EEDLY-----
Fd 2  IHQPEA------MGLSPDLQRQGYALLCVSYAQSDLEVETQD--------EDEVYELQFG
Fd 3  AEQADG------MGVSAELQAEGYALLCVAYPRSDLKIITED--------EVYQRQFGGQ
Fd 4  VEHTDKG----SDFLKPEELAAGCVLLCAAYATSDCKILTHQ--------EEALFG----
                                 *     .:  :            *

                 RNA polymerase Rpb1
Fd 5  AEENILNPRDGSILVEKGKLITRSMISQLDDQLQAAKIQIVNDTDE
Fd 1  ----------------------------------------------
Fd 2  RYFGAGRVRLGLPLDED-----------------------------
Fd 3  G---------------------------------------------
Fd 4  ---------- -----------------------------------
```

Fig. 5. Sequence alignment of Fd5 (Slr1048) with the plant-type [2Fe-2S] ferredoxins of *Synechocystis* 6803: Fd1 (Ssl0020), Fd2 (Sll1382), Fd3 (Slr1828) and Fd4 (Slr0150). Detected domains are marked on top of sequences. Conserved cysteines forming the 2Fe-2S cluster are shown in bold. Positions of T18 and T72 phosphorylation sites in Fd5 are marked with arrows, corresponding residues in other sequences are highlighted by bold and underlined.

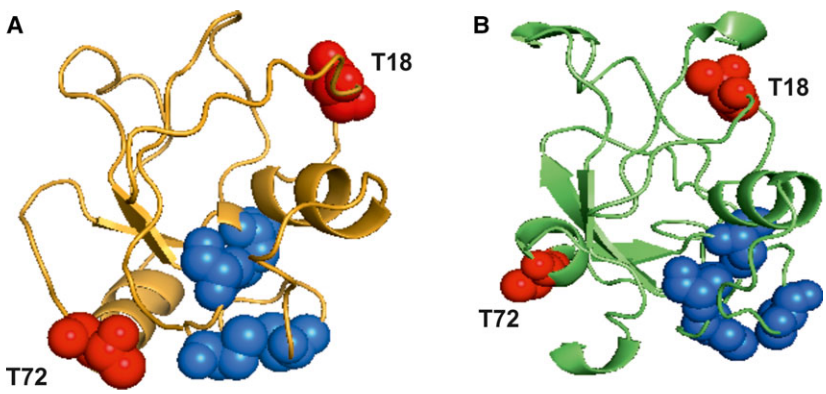

Fig. 6. 3D models of Fd5 from *Synechocystis* 6803 based on crystal structure of (A) putidaredoxin of *Pseudomonas putida* (4JWS.1.B) and (B) Fd1 from *Synechocystis* 6803 (1OFF). Positions of T18 and T72 are shown by red balls; positions of C residues coordinating the 2Fe-2S cluster are shown by blue balls.

T18 in the Δ*spkG* mutant is likely attributed to another S/T protein kinase of *Synechocystis* 6803.

The physiological role of the Fd5 protein in *Synechocystis* 6803 and, in particular, of phosphorylation on its two threonine residues still remains obscure. The sequence alignment (Fig. 5) revealed that introduction of negative charges on T18 and T72 increases the similarity of Fd5 to plant-type 2Fe-2S ferredoxins. Since, according to the 3D model (Fig. 6), the phosphorylation-dependent negative charges are most likely located on the opposite sides of the Fd5 protein, it is conceivable that the protein–protein interactions differ whether Fd5 is in phosphorylated or in nonmodified form. In addition to the canonical ferredoxin function, it is possible that the phospho-Fd5 serves as a link between two proteins in some still unknown molecular mechanism.

Wegener *et al*. [20] described the *slr0144–slr1052* gene cluster as the PAP operon. In contrast, Singh *et al*. [28] noted that *slr0151* and *slr0152* are not regulated together with the other seven genes. The separate expression of these two genes from the *slr1044–slr0150* operon was directly shown by Mitschke *et al*. [21] who analysed the transcriptomics organization of the entire *Synechocystis* genome, and was corroborated by Yang *et al*. [30] at the protein level. We observed that elimination of the SpkG kinase resulted in a significant decrease in the expression of the Slr0151 protein (Fig. 4B) which could be due to destabilization of bicistronic mRNA transcribed from the *slr0151–slr0152* operon.

Surprisingly, we observed that the knockout of the other gene in the *slr0151–slr0152* operon, resulting in elimination of the Slr0151 protein, caused an increase in Fd5 phosphorylation at both sites as compared to WT, and also slightly decreased the general level of Fd5 expression (Figs 3 and 4A). Thus, both proteins encoded by *slr0151–slr0152* affect Fd5. It is of note that the *slr0151* deletion did not disturb transcription of *spkG* (Fig. S2), most probably since the DNA region upstream the start codon of *slr0151* as well as the sequence encoding the C-terminal part of Slr0151 remained untouched in the *Δslr0151* mutant (Fig. 1).

While the function of the SpkG kinase in Fd5 phosphorylation is evident, the mechanism how Slr0151 stimulates this process is unclear. The Slr0151 protein does not have homology with protein phosphatases. It has been previously assigned to assist in regulation of the D1 *de novo* synthesis and photosystem II (PSII) disassembly/assembly under high light stress [30,31] as well as to play an important role in the assembly of photosystem I (PSI) [32]. Our results indicate that Slr0151 has yet another function determining the optimal ratio between phosphorylated and nonphosphorylated forms of Fd5, namely preventing its overphosphorylation. Indeed, when the Slr0151 protein is absent (Δ*slr0151*), distinct increase in Fd5 phosphorylation is evident as compared to WT. On the other hand, deletion of *spkG* (Δ*slr0152*) that eliminates Fd5 phosphorylation, concomitantly induces a significant drop in the amount of the Slr0151 protein. Is this novel function of Slr0151 related to assembly processes of photosystems or not remains an open question since neither Fd5 nor SpkG were found to be associated with PSI or PSII [30,32].

The existence of auxiliary proteins regulating the levels of protein phosphorylation is well documented in literature. For example, the Ssl3451 protein enhances autophosphorylation of Hik33 kinase in *Synechocystis* 6803 [33]; the effect is conserved in *Synechococcus* [34]. Similarly, auxiliary proteins have been reported for other organisms, like *E. coli* [35], *Bacillus subtilis* [36], *Vibrio cholerae* [37] etc. We propose that the Slr0151 protein functions as an auxiliary protein in regulation of the ratio between phosphorylated and nonphosphorylated forms of Fd5. The exact mechanism how the regulation is administered remains unknown but it is possible that the TPR motif present in the Slr0151 protein might play a role in this process.

The interplay among Fd5, the SpkG kinase and the Slr0151 protein described here sheds light on the complicated protein phosphorylation network in *Synechocystis* 6803 and expands our knowledge about involvement of auxiliary proteins in protein kinase–phosphoprotein relationships. The function of such auxiliary proteins in tuning the balance between phosphorylated and nonmodified forms of a protein might be important for proper responses of cyanobacteria to environmental signals. In addition, auxiliary proteins could provide an additional level of regulation for specific interactions of few protein kinases with numerous target proteins revealed by phosphoproteomic studies.

Acknowledgements

The research leading to these results has received funding from the People Programme (Marie Curie Actions) of the European Union's Seventh Framework Programme FP7/2007–2013/under REA Grants Agreement no. 317184 (MA). This material reflects only the authors' views and the European Union is not liable for any use that may be made of the information therein. The authors also gratefully acknowledge the financial support from the Academy of Finland Centre of Excellence Project number 307335, the Academy of Finland Project number 303757 (EMA), the Russian Science Foundation grant number 14-24-00020 (AZ) and the Turku University Foundation project number 9925 (NB). MS analysis was performed at the Turku Proteomics Facility, University of Turku and Åbo Akademi University, supported by Biocenter Finland. Dr. Dalton Carmel is acknowledged for participation in construction of *Synechocystis* 6803 mutants.

Author contributions

NB designed the project; MA and NB performed experiments and analyzed the data; AZ participated in construction of the mutants; MA, NB, AZ and EMA discussed the results and wrote the manuscript.

References

1 Cohen P (2002) The origins of protein phosphorylation. *Nat Cell Biol* **4**, e127–e130.

2 Olsen JV, Blagoev B, Gnad F, Macek B, Kumar C, Mortensen P and Mann M (2006) Global, *in vivo*, and site-specific phosphorylation dynamics in signaling networks. *Cell* **127**, 635–648.

3 Humphrey SJ, James DE and Mann M (2015) Protein phosphorylation: a major switch mechanism for metabolic regulation. *Trends Endocrinol Metab* **26**, 676–687.
4 Thingholm TE, Jensen ON and Larsen MR (2009) Analytical strategies for phosphoproteomics. *Proteomics* **9**, 1451–1468.
5 Mijakovic I and Macek B (2012) Impact of phosphoproteomics on studies of bacterial physiology. *FEMS Microbiol Rev* **36**, 877–892.
6 Yang MK, Qiao ZX, Zhang WY, Xiong Q, Zhang J, Li T, Ge F and Zhao JD (2013) Global phosphoproteomic analysis reveals diverse functions of serine/threonine/tyrosine phosphorylation in the model cyanobacterium *Synechococcus* sp. strain PCC 7002. *J Proteome Res* **12**, 1909–1923.
7 Chen Z, Zhan J, Chen Y, Yang M, He C, Ge F and Wang Q (2015) Effects of phosphorylation of β subunits of phycocyanins on state transition in the model cyanobacterium *Synechocystis* sp. PCC 6803. *Plant Cell Physiol* **56**, 1997–2013.
8 Spät P, Maček B and Forchhammer K (2015) Phosphoproteome of the cyanobacterium *Synechocystis* sp. PCC 6803 and its dynamics during nitrogen starvation. *Front Microbiol* **6**, 248.
9 Angeleri M, Muth-Pawlak D, Aro EM and Battchikova N (2016) Study of O-phosphorylation sites in proteins involved in photosynthesis-related processes in *Synechocystis* sp. strain PCC 6803: application of the SRM approach. *J Proteome Res* **15**, 4638–4652.
10 Soufi B, Gnad F, Jensen PR, Petranovic D, Mann M, Mijakovic I and Macek B (2008) The Ser/Thr/Tyr phosphoproteome of *Lactococcus lactis* IL1403 reveals multiply phosphorylated proteins. *Proteomics* **8**, 3486–3493.
11 Silva-Sanchez C, Li H and Chen S (2015) Recent advances and challenges in plant phosphoproteomics. *Proteomics* **15**, 1127–1141.
12 Zhu L and Li N (2012) Quantitation, networking, and function of protein phosphorylation in plant cell. *Front Plant Sci* **3**, 302.
13 Kamei A, Yuasa T, Geng X and Ikeuchi M (2002) Biochemical examination of the potential eukaryotic-type protein kinase genes in the complete genome of the unicellular cyanobacterium *Synechocystis* sp. PCC 6803. *DNA Res* **9**, 71–78.
14 Zorina A, Stepanchenko N, Novikova GV, Sinetova M, Panichkin VB, Moshkov IE, Zinchenko VV, Shestakov SV, Suzuki I, Murata N *et al.* (2011) Eukaryotic-like Ser/Thr protein kinases SpkC/F/K are involved in phosphorylation of GroES in the cyanobacterium *Synechocystis*. *DNA Res* **18**, 137–151.
15 Kamei A, Yuasa T, Orikawa K, Geng XX and Ikeuchi M (2001) A eukaryotic-type protein kinase, SpkA, is required for normal motility of the unicellular cyanobacterium S*ynechocystis* sp. strain PCC 6803. *J Bacteriol* **183**, 1505–1510.
16 Panichkin VB, Arakawa-Kobayashi S, Kanaseki T, Suzuki I, Los DA, Shestakov SV and Murata N (2006) Serine/threonine protein kinase SpkA in *Synechocystis* sp. strain PCC 6803 is a regulator of expression of three putative pilA operons, formation of thick pili, and cell motility. *J Bacteriol* **188**, 7696–7699.
17 Kamei A, Yoshihara S, Yuasa T, Geng X and Ikeuchi M (2003) Biochemical and functional characterization of a eukaryotic-type protein kinase, SpkB, in the cyanobacterium, *Synechocystis* sp. PCC 6803. *Curr Microbiol* **46**, 0296–0301.
18 Galkin AN, Mikheeva LE and Shestakov SV (2003) The insertional inactivation of genes encoding eukaryotic-type serine/threonine protein kinases in the cyanobacterium *Synechocystis* sp. PCC 6803. *Microbiology* **72**, 52–57.
19 Liang C, Zhang X, Chi X, Guan X, Li Y, Qin S and bo Shao H (2011) Serine/threonine protein kinase SpkG is a candidate for high salt resistance in the unicellular cyanobacterium *Synechocystis* sp. PCC 6803. *PLoS ONE* **6**, e18718.
20 Wegener KM, Welsh EA, Thornton LE, Keren N, Jacobs JM, Hixson KK, Monroe ME, Camp DG, Smith RD and Pakrasi HB (2008) High sensitivity proteomics assisted discovery of a novel operon involved in the assembly of photosystem II, a membrane protein complex. *J Biol Chem* **283**, 27829–27837.
21 Mitschke J, Georg J, Scholz I, Sharma CH, Dienst D, Bantscheff J, Voß B, Steglich C, Wilde A, Vogel J *et al.* (2011) An experimentally anchored map of transcriptional start sites in the model cyanobacterium *Synechocysti*s sp. PCC6803. *Proc Natl Acad Sci USA* **108**, 2124–2129.
22 Cassier-Chauvat C and Chauvat F (2014) Function and regulation of ferredoxins in the cyanobacterium, *Synechocystis* PCC6803: recent advances. *Life* **4**, 666–680.
23 Rippka R (1988) Isolation and purification of cyanobacteria. *Meth Enzymol* **167**, 3–27.
24 Mustila H, Allahverdiyeva Y, Isojärvi J, Aro EM and Eisenhut M (2014) The bacterial-type [4Fe–4S] ferredoxin 7 has a regulatory function under photooxidative stress conditions in the cyanobacterium *Synechocystis* sp. PCC 6803. *Biochim Biophys Acta* **1837**, 1293–1304.
25 Pollari M, Ruotsalainen V, Rantamäki S, Tyystjärvi E and Tyystjärvi T (2009) Simultaneous inactivation of sigma factors B and D interferes with light acclimation of the cyanobacterium *Synechocystis* sp. strain PCC 6803. *J Bacteriol* **191**, 3992–4001.
26 MacLean B, Tomazela DM, Shulman N, Chambers M, Finney GL, Frewen B, Kern R, Tabb DL, Liebler DC and MacCoss MJ (2010) Skyline: an open source

document editor for creating and analyzing targeted proteomics experiments. *Bioinformatics* **26**, 966–968.

27 Hall TA (1999) BioEdit: a user-friendly biological sequence alignment editor and analysis program for Windows 95/98/NT. *Nucleic Acids Symp Ser* **41**, 95–98.

28 Singh AK, Li H and Sherman LA (2004) Microarray analysis and redox control of gene expression in the cyanobacterium *Synechocystis* sp. PCC 6803. *Physiol Plant* **120**, 27–35.

29 Picotti P and Aebersold R (2012) Selected reaction monitoring-based proteomics: workflows, potential, pitfalls and future directions. *Nat Methods* **9**, 555–566.

30 Yang H, Liao L, Bo T, Zhao L, Sun X, Lu X, Norling B and Huang F (2014) Slr0151 in *Synechocystis* sp. PCC 6803 is required for efficient repair of photosystem II under high-light condition. *J Integr Plant Biol* **56**, 1136–1150.

31 Rast A, Rengstl B, Heinz S, Klingl A and Nickelsen J (2016) The role of Slr0151, a tetratricopeptide repeat protein from *Synechocystis* sp. PCC 6803, during Photosystem II assembly and repair. *Front Plant Sci* **7**, 605.

32 Kubota H, Sakurai I, Katayama K, Mizusawa N, Ohashi S, Kobayashi M, Zhang P, Aro EM and Wada H (2010) Purification and characterization of photosystem I complex from *Synechocystis* sp. PCC 6803 by expressing histidine-tagged subunits. *Biochim Biophys Acta* **1797**, 98–105.

33 Sakayori T, Shiraiwa Y and Suzuki I (2009) A *Synechocystis* homolog of SipA protein, Ssl3451, enhances the activity of the histidine kinase Hik33. *Plant Cell Physiol* **50**, 1439–1448.

34 Espinosa J, Fuentes I, Burillo S, Rodriguez-Mateos F and Contreras A (2006) SipA, a novel type of protein from *Synechococcus* sp. PCC 7942, binds to the kinase domain of NblS. *FEMS Microbiol Lett* **254**, 41–47.

35 Wanner BL (1993) Gene regulation by phosphate in enteric bacteria. *J Cell Biochem* **51**, 47–54.

36 Szurmant H, Nelson K, Kim EJ, Perego M and Hoch JA (2005) YycH regulates the activity of the essential YycFG two-component system in *Bacillus subtilis*. *J Bacteriol* **187**, 5419–5426.

37 Mitchell SL, Ismail AM, Kenrick SA and Camilli A (2015) The VieB auxiliary protein negatively regulates the VieSA signal transduction system in *Vibrio cholerae*. *BMC Microbiol*, **15**, 59.

Supporting information

Additional Supporting Information may be found online in the supporting information tab for this article:

Fig. S1. Confirmation of the complete segregation in (A) the *ΔspkG* mutant (0.9% agarose gel) and (B) the Δ*slr0151* mutant (1% agarose gel). M, DNA markers, 1-Kb ladder.

Fig. S2. Expression of the *spkG* gene at the transcriptional level in WT and *Δslr0151* strains determined by RT-qPCR.

Fig. S3. Sequence alignment of Fd5 from *Synechocystis* 6803 with the orthologous proteins in other cyanobacteria possessing the PAP operon: Cya_1946 in *Synechococcus* sp. JA-3-3Ab, Cyb_0815 in *Synechococcus* sp. JA-2-3B'a(2–13), Tlr2302 in *Thermosynechococcus elongatus* BP-1, Cce_2108 in *Cyanothece* sp. ATCC 51142 and Cwat 4335 from *Crocosphaera watsonii* WH 8501. Conserved cysteines forming the 2Fe-2S cluster are shown in bold. Positions of conserved phosphorylated threonines are marked with arrows, highlighted by bold and underlined.

Table S1. Sequences of PCR primers used for construction of the Δ*slr0152* and Δ*slr0151* mutants. Restriction sites introduced into the PCR fragments are shown in bold.

Table S2. SRM quantification data extracted from the Skyline file https://panoramaweb.org/labkey/SpkG-Fd5-SYN_GT.url; RT: Retention time.

Table S3. Calculations of relative peptide abundances in *Δslr0152* and *Δslr0151* strains compared to WT based on data in Table S2.

Doc S1. https://panoramaweb.org/SpkG-Fd5-SYN_GT.url